

Synthesis Crystal Structure and Magnetic Properties of the Trinuclear Nickel(II) Complex Bis[(μ -thiocyanato-*N*)bis(μ -pyridazine-*N*¹,*N*²)-bis(thiocyanato-*N*)(pyridazine-*N*¹)nickel(II)-*N*,*N*¹,*N*^{1'}]nickel(II)

Juan Cano,^{1a} Giovanni De Munno,^{*1b}
Francesc Lloret,^{*1a} and Miguel Julve^{1a}

Departament de Química Inorgànica, Facultat de Química de la Universitat de València, Dr. Moliner 50, 46100 Burjassot, València, Spain, and Dipartimento di Chimica dell'Università degli Studi della Calabria, 87030 Arcavacata di Rende, Cosenza, Italy

Received October 18, 1999

Introduction

Heterocyclic diazines such as pyridazine commonly act as exo-bidentate ligands toward metal ions, yielding polynuclear compounds whose nuclearity can be controlled by introducing appropriate substituents on the diazine ring, using suitable end-cap ligands or anions of different donor abilities.^{2–11} As a bridging ligand, pdz offers a short two-atom pathway for the exchange coupling. In fact, strong antiferromagnetic interactions between copper(II) ions singly and doubly bridged by pdz ligands have been observed.^{8,12} In the case of nickel(II), a moderate antiferromagnetic coupling, $J = -33.6 \text{ cm}^{-1}$ (the Hamiltonian being defined as $\hat{H} = -J\hat{S}_A \cdot \hat{S}_B$), was observed recently in a structurally characterized nickel(II) dimer where two substituted pdz-type ligands act as bridges.¹⁰

A more interesting situation from a magnetic point of view arises when a pseudohalide anion and the diazine group act as bridges simultaneously. For dinuclear copper(II) complexes with end-on azido and diazine bridges, a very strong antiferromagnetic coupling was observed (J ca. -800 cm^{-1}) for angles at the azido bridge close to 120° .^{13,14} The complementarity of these bridging ligands accounts for the nature and magnitude of the

coupling observed.^{15,16} For the linear and centrosymmetric trinuclear nickel(II) complex of formula $[\text{Ni}_3(\text{detrH})_6(\text{NCS})_6] \cdot 2\text{H}_2\text{O}$ (**2**) (detrH = 3,5-diethyl-1,2,4-triazole) with an end-on *N*-thiocyanato group and two bismonodentate triazoles as bridges the magnetic coupling is weakly ferromagnetic.¹⁷ In the latter case, the antiferromagnetic coupling through the diazine pathway is overcome by the ferromagnetic one through the unusual end-on thiocyanato bridge, leading to a net ferromagnetic coupling between adjacent metal ions.

In the present contribution we report the preparation and the structural and magnetic characterization of the centrosymmetric trinuclear nickel(II) complex of formula $[\text{Ni}_3(\text{pdz})_6(\text{NCS})_6]$ (**1**) (pdz = pyridazine). This is a rare case where the compensation between the antiferromagnetic (through double pdz bridges) and ferromagnetic (through a single end-on thiocyanato bridge) interactions account for the quasi Curie law behavior observed.

Experimental Section

Materials. Nickel(II) perchlorate hexahydrate, potassium thiocyanate, and pyridazine were purchased from commercial sources and used as received. Elemental analysis (C, H, N, S) were performed by the Microanalytical Service of the Universidad Autónoma de Madrid.

Preparation of $[\text{Ni}_3(\text{pdz})_6(\text{NCS})_6]$ (1**).** A methanolic solution of nickel(II) thiocyanate (1 mmol, 100 mL) was prepared by mixing solutions containing stoichiometric amounts of nickel(II) perchlorate (0.366 g, 1 mmol) and potassium thiocyanate (0.194 g, 2 mmol). After removal of the white precipitate of the potassium perchlorate by filtration, a methanolic solution (5 mL) of pyridazine (0.160 g, 2 mmol) was added dropwise under continuous stirring. Single crystals of **1** as pale purple prisms were grown from the blue-greenish mother liquor by slow evaporation at room temperature. The yield is ca. 90%. Anal. Calcd for $\text{C}_{30}\text{H}_{24}\text{Ni}_3\text{N}_{18}\text{S}_6$ (**1**): C, 35.90; H, 2.39; N, 25.08; S, 19.15. Found: C, 35.81; H, 2.31; N, 24.89; S, 19.04.

The most interesting features of the infrared spectra of **1** concern the bands close to 2000 cm^{-1} , which can be assigned to the ν_{CN} of the thiocyanate ligand. The occurrence of two strong peaks at ca. 2075 and 1966 cm^{-1} is in agreement with the presence of terminal N-bonded and end-on N-bridging thiocyanates. In light of previous data on structurally characterized compounds containing these two types of thiocyanate ligands,¹⁷ it can be concluded that the low CN stretching frequency of the IR spectra of **1** is diagnostic for a NCS ligand exhibiting the unusual end-on N-bridging mode.

Physical Techniques. The IR spectrum was recorded on a Nicolet Impact 410 spectrometer as a KBr pellet in the $4000\text{--}400 \text{ cm}^{-1}$ region. Magnetic susceptibility measurements were carried out on a polycrystalline sample in the temperature range 1.9–300 K under a magnetic field of 0.1 T by using a Quantum Design SQUID magnetometer. The susceptometer was calibrated with $(\text{NH}_4)_2\text{Mn}(\text{SO}_4)_2 \cdot 12\text{H}_2\text{O}$. Diamagnetic corrections were estimated from Pascal's constants¹⁸ and found to be $-492 \times 10^{-6} \text{ cm}^3 \text{ mol}^{-1}$. The magnetic susceptibility data were also corrected for the temperature-independent paramagnetism ($-100 \times 10^{-6} \text{ cm}^3 \text{ mol}^{-1}$ per nickel(II)).

X-ray Crystallographic Analysis. Diffraction data of a crystal of **1** of dimensions $0.25 \times 0.30 \times 0.48 \text{ mm}$ were collected on a Siemens R3m/V automatic diffractometer by using graphite-monochromatized Mo K α radiation and the ω - 2θ scan technique. Unit cell dimensions

- * To whom correspondence should be addressed.
(1) (a) Universitat de València. (b) Università degli Studi della Calabria.
(2) Inoue, M.; Kubo, N. *Coord. Chem. Rev.* **1976**, *21*, 1.
(3) Reedijk, J. In *Comprehensive Coordination Chemistry*; Wilkinson, G., Gillard, R. D., McCleverty, J. A., Eds.; Pergamon Press: New York, 1987; Vol. 2, p 73.
(4) Steel, P. J. *Coord. Chem. Rev.* **1990**, *106*, 227.
(5) Drew, M. G. B.; Yates, P. C.; Trocha-Grimshaw, J.; Lavery, A.; McKillop, K. P.; Nelson, S. M.; Nelson, J. J. *Chem. Soc., Dalton Trans.* **1988**, 347.
(6) Fetzer, T.; Lentz, A.; Debaerdemaeker, T.; Abou-El-Wafa, O. Z. *Naturforsch. B* **1990**, *45*, 199.
(7) (a) Carlucci, L.; Gianfranco, C.; Moret, M.; Sironi, A. J. *Chem. Soc., Dalton Trans.* **1994**, 2397. (b) Masciocchi, N.; Cairati, P.; Carlucci, L.; Ciani, G.; Mezza, G.; Sironi, A. J. *Chem. Soc., Dalton Trans.* **1994**, 3009.
(8) (a) Otieno, T.; Rettig, S. J.; Thompson, R. C.; Trotter, J. *Inorg. Chem.* **1993**, *32*, 4384. (b) Otieno, T.; Rettig, S. J.; Thompson, R. C.; Trotter, J. *Inorg. Chem.* **1995**, *34*, 1718.
(9) Li, C.; Kanehisa, N.; Miyagi, Y.; Nakao, Y.; Takamizawa, S.; Mori, W.; Kai, Y. *Bull. Chem. Soc. Jpn.* **1977**, *70*, 2429.
(10) Escuer, A.; Vicente, R.; Mernari, B.; El Gueddi, A.; Pierrot, M. *Inorg. Chem.* **1997**, *36*, 2511.
(11) Tandon, S. S.; Thompson, L. K.; Haynes, R. C. *Inorg. Chem.* **1992**, *31*, 2210.
(12) Emori, S.; Inoue, M.; Kubo, M. *Bull. Chem. Soc. Jpn.* **1972**, *45*, 2259.
(13) Tandon, S. S.; Thompson, L. K.; Manuel, M. E.; Bridson, J. N. *Inorg. Chem.* **1994**, *33*, 5555.

- (14) Thompson, L. K.; Tandon, S. S.; Manuel, M. E. *Inorg. Chem.* **1995**, *34*, 2356.
(15) Thompson, L. K.; Tandon, S. S.; Lloret, F.; Cano, J.; Julve, M. *Inorg. Chem.* **1997**, *36*, 3301.
(16) Kahn, O. *Molecular Magnetism*; VCH: New York, 1993; p 164.
(17) van Albada, G. A.; de Graaf, R. A. G.; Haasnoot, J. G.; Reedijk, J. *Inorg. Chem.* **1984**, *23*, 1404.
(18) Earnshaw, A. *Introduction to Magnetochemistry*; Academic Press: London and New York, 1968.

Table 1. Crystal Data for $[\text{Ni}_3(\text{pdz})_6(\text{NCS})_6]$ (**1**)

formula	$\text{C}_{30}\text{H}_{24}\text{N}_{18}\text{Ni}_3\text{S}_6$
fw	1005.2
space group	$P2_1/n$ (No. 14)
a , Å	8.059(3)
b , Å	18.074(4)
c , Å	14.259(3)
β , deg	100.36(3)
V , Å ³	2043.1(11)
Z	2
T , K	295
ρ_{calc} , g cm ⁻³	1.634
λ , Å	0.71073 Å
$\mu(\text{Mo K}\alpha)$, cm ⁻¹	17.24
R^a	0.055
R_w^b	0.057

$$^a R = \sum(|F_o| - |F_c|) / \sum|F_o|. \quad ^b R_w = [\sum w(|F_o| - |F_c|)^2 / \sum w|F_o|^2]^{1/2}.$$

and orientation matrixes were obtained from least-squares refinement of 25 strong reflections in the $15^\circ \leq 2\theta \leq 30^\circ$ range. A summary of the crystallographic data and structure refinement is given in Table 1. A total of 4955 reflections were collected in the range $3^\circ \leq 2\theta \leq 54^\circ$; 4447 of them were unique, and from these, 2558 were assumed as observed ($I \geq 3\sigma(I)$) and used for the refinement of the structure. Examination of three standard reflections, monitored every 100, showed no sign of crystal deterioration. Lorentz, polarization, and analytical absorption corrections¹⁹ were applied to the intensity data. The maximum and minimum transmission factors were 0.759 and 0.344.

The structure of **1** was solved by standard Patterson methods with the SHELXTL-PLUS program²⁰ and subsequently completed by Fourier recycling. All non-hydrogen atoms were refined anisotropically. The hydrogen atoms were set in calculated positions and refined as riding atoms with a common fixed isotropic thermal parameter. The full-matrix least-squares refinements were carried out by minimizing the function $\sum w(|F_o| - |F_c|)^2$ with $w = 1/[\sigma^2(F_o) + 0.0009(F_o)^2]$. Models reached convergence with values of the R and R_w indices listed in Table 1. The goodness of fit value was 1.55. Residual maximum and minimum in the final difference map were 0.91 and $-0.60 \text{ e } \text{Å}^{-3}$. The final geometrical calculations and graphical manipulations were carried out with the PARST program²¹ and the XP utility of the SHELX-PLUS system, respectively. Selected bond distances and angles are listed in Table 2.

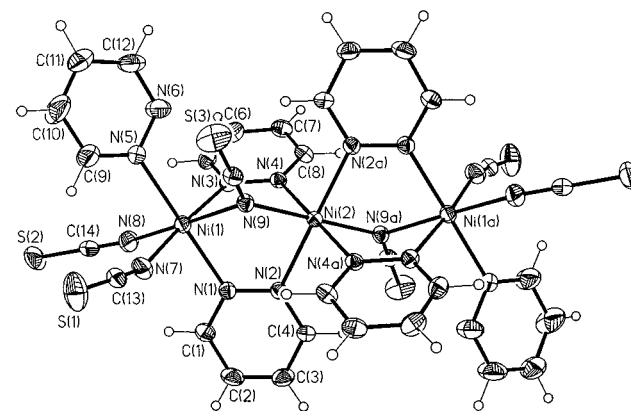
Results and Discussion

Crystal Structure. The structure of **1** consists of neutral trimeric, centrosymmetric complex molecules of formula $[\text{Ni}_3(\text{pdz})_6(\text{NCS})_6]$ (Figure 1). The two crystallographically independent nickel atoms (Ni(1) and Ni(2)) exhibit a somewhat distorted octahedral NiN_6 environment. The central nickel(II) ion (Ni(2)) is surrounded by four bridging pdz ligands and two thiocyanate groups in trans positions. These two thiocyanate groups exhibit the end-on bridging mode through the nitrogen atom. This is a rare coordination mode of the thiocyanate ligand given the small number of structurally characterized complexes where it occurs.^{17,22–27} The two unique Ni(2)–N(pdz) bond

Table 2. Selected Bond Lengths (Å) and Angles (deg)^{a,b} for Compound **1**

Ni(1)–N(1)	2.096(5)	Ni(1)–N(3)	2.134(5)
Ni(1)–N(5)	2.135(6)	Ni(1)–N(7)	2.038(6)
Ni(1)–N(8)	2.051(5)	Ni(1)–N(9)	2.158(4)
Ni(2)–N(2)	2.121(4)	Ni(2)–N(4)	2.119(4)
Ni(2)–N(9)	2.066(5)		
N(1)–Ni(1)–N(3)	88.5(2)	N(1)–Ni(1)–N(5)	178.5(2)
N(3)–Ni(1)–N(5)	92.0(2)	N(1)–Ni(1)–N(7)	88.9(2)
N(3)–Ni(1)–N(7)	174.7(2)	N(5)–Ni(1)–N(7)	90.6(2)
N(1)–Ni(1)–N(8)	93.1(2)	N(3)–Ni(1)–N(8)	92.1(2)
N(5)–Ni(1)–N(8)	88.4(2)	N(7)–Ni(1)–N(8)	92.7(2)
N(1)–Ni(1)–N(9)	86.8(2)	N(3)–Ni(1)–N(9)	84.9(2)
N(5)–Ni(1)–N(9)	91.8(2)	N(7)–Ni(1)–N(9)	90.4(2)
N(8)–Ni(1)–N(9)	177.0(2)	N(2)–Ni(2)–N(4)	91.5(2)
N(2)–Ni(2)–N(9)	87.2(2)	N(4)–Ni(2)–N(9)	86.3(2)
N(4)–Ni(2)–N(2a)	88.5(2)	N(9)–Ni(2)–N(2a)	92.8(2)
N(2)–Ni(2)–N(4a)	88.5(2)	N(9)–Ni(2)–N(4a)	93.7(2)
N(2)–Ni(2)–N(9a)	92.8(2)	N(4)–Ni(2)–N(9a)	93.7(2)
Ni(1)–N(9)–Ni(2)	105.4(2)		

^a Estimated standard deviations in the last significant digits are given in parentheses. ^b Symmetry code: (a) $-x, -y, -z$.

**Figure 1.** Perspective drawing of **1** along with the atom labeling. Thermal ellipsoids are drawn at the 30% probability level.

distances are practically identical (2.121(4) and 2.119(4) Å) and somewhat longer than the Ni(2)–N(thiocyanate) bond length (2.066(5) Å). The peripheral nickel atoms (Ni(1) and Ni(1a)) are bonded to three bridging nitrogens (two from pdz and one from NCS⁻) and three terminal ones (two monodentate NCS groups and one monodentate pdz ligand). The Ni(1)–N(thiocyanate) bonds occur in two sets, the terminal ones (2.038(6) and 2.051(5) Å) being significantly shorter than that of the bridge (2.158(4) Å). The Ni(1)–N(pdz) bonds vary in the range 2.135(6)–2.096(5) Å. The largest deviation from the ideal octahedral geometry in the N–Ni–N bond angles is 5.1° at Ni(1) and 3.7° at Ni(2). The best equatorial plane around Ni(1) is defined by the N(3), N(9), N(7), and N(8) atoms [the largest deviation from the mean plane is 0.025(6) Å for N(7) and the nickel atom is 0.022(3) Å out of this plane], whereas all the planes of the octahedron around Ni(2) are perfectly planar and the metal ion lies in these planes. The planes defined by the N(3)N(9)N(7)N(8) and N(4)N(9)N(4a)N(9a) sets of atoms form a dihedral angle of 52.9(1)°. The pdz rings are found to be planar within experimental error, and the intra-ring bond distances and angles compare well with those previously reported.^{5–9,12} The dihedral angle between the two bridging pdz ligands is 69.5–(2)°. The terminal pdz ligand forms dihedral angles of 42.1(2)° and 64.7(2)° with the bridging pdz groups.

The thiocyanate ligands are quasi linear [the values of the N–C–S bond angle ranging from 177.9(6)° to 178.5(7)°],

- (19) North, A. C. T.; Philips, D. C.; Mathews, F. S. *Acta Crystallogr.* **1968**, *A24*, 351.
 (20) SHELX-PLUS, Version 4.21/V; Siemens Analytical X-Ray Instruments Inc.: Madison, WI, 1990.
 (21) Nardelli, M. *Comput. Chem.* **1983**, *7*, 95.
 (22) Cotton, F. A.; Davison, A.; Ilesley, W. H.; Trop, H. S. *Inorg. Chem.* **1979**, *18*, 2719.
 (23) Groevenheld, L. R.; Vos, G.; VErschoor, G. C.; Reedijk, J. *J. Chem. Soc., Chem. Commun.* **1982**, 620.
 (24) Harding, P. A.; Henrick, K.; Lindoy, L. F.; McPartlin, M.; Tasker, P. A. *J. Chem. Soc., Chem. Commun.* **1983**, 1300.
 (25) Drew, M. G. B.; Esho, F. S.; Nelson, S. M. *Inorg. Chim. Acta* **1983**, *76*, L269.
 (26) Brooker, S.; Kelly, J. R. *J. Chem. Soc., Dalton Trans.* **1996**, 2117.
 (27) Mohanta, S.; Nanda, K. K.; Werner, R.; Haase, W.; Mukherjee, A. K.; Dutta, S. K.; Nag, K. *Inorg. Chem.* **1997**, *36*, 4656.

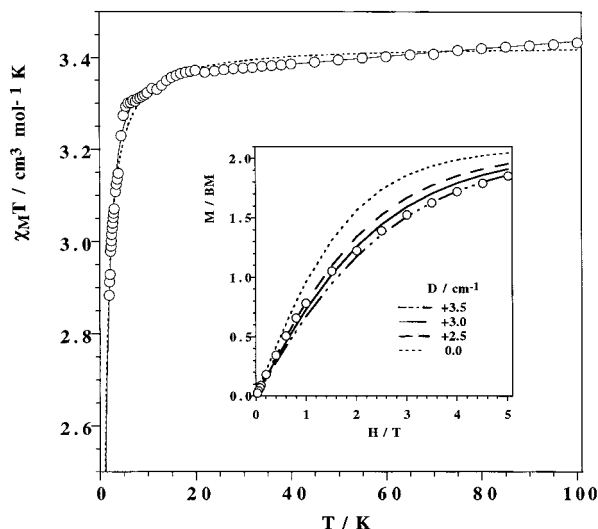


Figure 2. $\chi_M T$ versus T plot for **1**: (O) experimental data; (○) and (—) best-fit curve through eqs 1 and 2, respectively. The inset shows the magnetization curve at 1.9 K: (O) experimental data; (○), (---), (—), and (· · · · ·) best fit curves with $D = 3.5, 3.0, 2.5,$ and 0.0 cm^{-1} , respectively.

whereas a significant bending is displayed by the terminal Ni(1)–N–C(S) linkages [$158.8(6)^\circ$ and $158.1(6)^\circ$ for Ni(1)–N(8)–C(14) and Ni(1)–N(7)–C(13), respectively].

The nearest-neighbor Ni···Ni distance within the trimeric molecule is $3.362(1) \text{ \AA}$, a value quite close to that reported for the trinuclear $[\text{Ni}_3(\text{detrH})_6(\text{NCS})_6] \cdot 2\text{H}_2\text{O}$ (**2**) complex ($3.39(1) \text{ \AA}$),¹⁷ where two bridging triazole and one N-bridging thiocyanate ligand occur. The shortest intermolecular metal–metal separation in **1** is $8.059(3) \text{ \AA}$ [Ni(1)···Ni(1b) and Ni(2)···Ni(2b); (b) = 1 + x, y, z]. The trimeric molecules exhibit very weak π – π intermolecular interactions (ca. 4 \AA) between terminal pdz ligands.

Magnetic Properties of 1. The thermal dependence of $\chi_M T$ (χ_M being the magnetic susceptibility per mol of trimer) for the title complex in the temperature range 1.9–100 K is shown in Figure 2. The value of $\chi_M T$ at room temperature ($3.45 \text{ cm}^3 \text{ mol}^{-1} \text{ K}$) corresponds to what is expected for three noninteracting single-ion triplet states. This value remains practically unchanged down to 20 K and then decreases quickly to $2.88 \text{ cm}^3 \text{ mol}^{-1} \text{ K}$ at 1.9 K. This low-temperature decrease could be due to weak antiferromagnetic coupling, single-ion zero-field interactions (D), or both. Taking into account the discrete trimeric structure of **1**, in a first approach we tried to fit its magnetic behavior through the isotropic spin Hamiltonian defined by eq 1:

$$\hat{H} = -J[(\hat{S}_1 \cdot \hat{S}_2) + (\hat{S}_2 \cdot \hat{S}_3)] \quad (1)$$

with $S_1 = S_2 = S_3 = 1$ and assuming that $g_x = g_y = g_z = g$. J represents the magnetic interaction between adjacent metal ions within the trimer. Least-squares fit through eq 1 leads to $J = -0.24 \text{ cm}^{-1}$, $g = 2.13$, and $R = 2.6 \times 10^{-5}$ (R is the agreement factor defined as $\sum_i [(\chi_M T)^{\text{exptl}}(i) - (\chi_M T)^{\text{calc}}(i)]^2 / \sum_i [(\chi_M T)^{\text{exptl}}(i)]^2$). In a second step we have attempted to fit the magnetic properties of **1** through the Hamiltonian of eq 2,

$$\hat{H} = D(\hat{S}_{z1}^2 + \hat{S}_{z2}^2 + \hat{S}_{z3}^2) \quad (2)$$

which takes into account the local axial anisotropy of the nickel(II) ions. Although the peripheral nickel atoms are not equivalent

to the central one, we have used a unique D parameter (zero field splitting) as well as a single isotropic g value as variables in order to avoid the overparametrization. The results of the least-squares fit through the corresponding theoretical expression lead to $|D| = 3.0 \text{ cm}^{-1}$, $g = 2.12$, and $R = 1.5 \times 10^{-5}$. An inspection of the fits in Figure 2 shows that a better match of the magnetic data of **1** is obtained through this last approach. When J , D , and g are used as variable parameters, the quality of the fit is not improved and the computed value of J is very small, indicating that D is the main parameter. The inset of Figure 2 shows the magnetization data as a function of the applied magnetic field together with the calculated curves with $g = 2.12$ and different D values. It can be seen there how the D value for **1** has to be comprised between 2.5 and 3.5 cm^{-1} , in agreement with the computed value of the fit of the magnetic data, which is given above. The occurrence of very small magnetic interactions and/or somewhat different D values for the two types of nickel(II) ions in **1** account for the small deviation of the fit for $D = 3.0 \text{ cm}^{-1}$.

In a recent work, the magnetic coupling in a nickel(II) dimer through double μ -1,2-pdz was found to be relatively strong antiferromagnetic ($J = -33.6 \text{ cm}^{-1}$).¹⁰ Given that the topology of the bridging pyridazine in this complex and in **1** is the same, one can conclude that the quasi Curie law behavior of **1** can be explained only by assuming that the magnetic coupling through the single end-on N -thiocyanato has to be ferromagnetic and very close to 33 cm^{-1} . So, the magnetic couplings through both types of bridges in **1** would cancel each other. In this respect, it is interesting to note that the magnetic coupling between adjacent nickel(II) ions in the linear trimeric compound **2** (where two 1,2-bridging triazole ligands and one end-on N -bridging thiocyanate occur between each pair of nickel atoms) is ferromagnetic ($J = +19.2 \text{ cm}^{-1}$).¹⁷ Since the triazole is able to mediate antiferromagnetic interactions of ca. -10.3 cm^{-1} in the triazole-bridged nickel(II) complexes,²⁸ it can be estimated that the exchange coupling through the single end-on N -thiocyanate bridge in **2** should be ca. $+30 \text{ cm}^{-1}$ ($J_2 = J_{\text{triazole}} + J_{\text{NCS}}$ with $J_{\text{triazole}} \approx 10 \text{ cm}^{-1}$ and $J_{\text{NCS}} \approx +30 \text{ cm}^{-1}$). The fact that the value of the angle at the thiocyanato bridge in **1** ($105.4(2)^\circ$) is identical to that observed in **2** ($105.5(5)^\circ$)¹⁷ allows us to assign a value of ca. $+30 \text{ cm}^{-1}$ to the magnetic coupling through the thiocyanato bridge in **1**.

As far as we know, there are no magneto-structurally characterized examples of N -bridged thiocyanato nickel(II) complexes to check our conclusions. However, it has been shown that other pseudohalides such as cyanato or azide are able to mediate significant ferromagnetic interactions between nickel(II) ions when adopting the end-on N -bridging mode.^{29,30} In the near future, more examples of dimers with end-on N -bridging thiocyanate should be investigated to characterize the ability of this kind of bridge to transmit ferromagnetic

(28) Antolini, L.; Fabretti, A. C.; Gatteschi, D.; Giusti, A.; Sessoli, R. *Inorg. Chem.* **1990**, *29*, 143.

(29) Arriortua, A. I.; Cortés, R.; Mesa, J. L.; Lezama, L.; Rojo, T.; Villeneuve, G. *Transition Met. Chem.* **1988**, *13*, 371.

(30) (a) Arriortua, A. I.; Cortés, R.; Lezama, L.; Rojo, T.; Solans, X.; Font-Bardia, *Inorg. Chim. Acta* **1990**, *174*, 263. (b) Escuer, A.; Vicente, R.; Ribas, J. *J. Magn. Magn. Mater.* **1992**, *110*, 181. (c) Cortés, R.; Ruiz de Laramendi, J. I.; Lezama, L.; Rojo, T.; Urtiaga, K.; Arriortua, M. I. *J. Chem. Soc., Dalton Trans.* **1992**, 2723. (d) Vicente, R.; Escuer, A.; Ribas, J.; El Fallah, M. S.; Solans, X.; Font-Bardia, M. *Inorg. Chem.* **1993**, *32*, 1920. (e) Escuer, A.; Vicente, R.; Ribas, J.; Solans, X. *Inorg. Chem.* **1995**, *34*, 1793. (f) Escuer, A.; Vicente, R.; Salah El Fallah, M.; Solans, X.; Font-Bardia, M. *Inorg. Chim. Acta* **1996**, *247*, 85.

coupling and to correlate its magnitude with structural factors, as has already been done for the parent azide ligand.³¹

Acknowledgment. Financial support from the Spanish Dirección General de Investigación Científica y Técnica (DGI-CYT) (Project PB97-1397), the Italian Ministero dell'Università e della Ricerca Scientifica e Tecnologica, and the Training and

Mobility Research Program from the European Community (TMR Contract ERBFMRXCT-980181) is gratefully acknowledged.

Supporting Information Available: X-ray crystallographic files in CIF format. This material is available free of charge via the Internet at <http://pubs.acs.org>.

(31) Ruiz, R.; Cano, J.; Alvarez, S.; Alemany, P. *J. Am. Chem. Soc.* **1998**, *120*, 11122.

IC991219L